J Electroceram (2006) 17:365–368
DOI 10.1007/s10832-006-7239-7

Pb cation induced low-temperature crystallization of (Ba·Pb) hexa-ferrite thin films

Seok Joo Doh · Jung Ho Je · Tae Sik Cho

Received: 29 June 2005 / Revised: 24 November 2005 / Accepted: 17 January 2006

Abstract We have studied the low-temperature crystallization of (Ba·Pb) hexa-ferrite thin films using real time synchrotron X-ray scattering, anomalous X-ray scattering, and vibrating sample magnetometer. The crystallization temperature of amorphous (Ba·Pb) hexa-ferrite film (300-Å-thick, ∼530°C) was much lower than that of amorphous Ba hexa-ferrite film, ∼750°C. The crystalline (Ba·Pb) hexa-ferrite phase was formed by solid phase transformation of the interfacial crystalline Fe_3O_4 phase through the diffusion of Ba or Pb cations. The low crystallization temperature of the (Ba·Pb) hexa-ferrite phase was due to the lower diffusion activation barrier of Pb cations than that of Ba cations. The small grain size (∼40 nm in diamter) and comparable magnetic properties ($Ms_\perp$: 337 emu/cm^3, $iHc_\perp$: 1.60 kOe) of the crystallized (Ba·Pb) hexa-ferrite film also demonstrate its potential possibility for high-density recording media.

Keywords Low temperature · Crystallization · Hexa-ferrite · Pb ions · Synchrotron X-ray

S.J. Doh
Advanced Nano Materials Research Team, Daegu Gyeongbuk Institute of Science and Technology, Daegu, 700-742, Korea

J.H. Je (✉)
Synchrotron X-ray Laboratory, Department of Materials Science and Engineering and Center for Information Materials, Pohang University of Science and Technology, Pohang, 790-784, Korea
e-mail: jhje@postech.ac.kr

T.S. Cho
Department of Materials Science and Engineering, Sangju National University, Sangju, 742-711, Korea

1 Introduction

For the application of magnetic recording and microwave circuit, researchers have focused on the Ba hexa-ferrite films mainly due to its large uniaxial anisotropy, excellent chemical stability, and high mechanical durability [1, 2]. Especially, due to its large uniaxial magnetic anisotropy (17 kOe) [3], Ba hexa-ferrite thin films have been extensively studied for perpendicular magnetic recording media [4].

However, it is essentially required to reduce the crystallization temperature of Ba hexa-ferrite for high-density magnetic recording media. The substrate temperature necessary for crystallization of Ba hexa-ferrite was ∼900°C, which is not compatible with most commercially used substrate materials such as glass [5]. Therefore, the substitution of Pb for Ba in the hexa-ferrite structure was investigated to reduce the crystallization temperature. Previous studies showed that the Pb substituted Ba hexa-ferrite film such as $PbFe_{12}O_{19}$ and $(Ba_{1-x}Pb_x)$ $Fe_{12}O_{19}$ film crystallized at a lower substrate temperature than Ba hexa-ferrite film [5, 6]. However, the role of substitutional Pb ions in the low-temperature crystallization and the crystallization behavior of Pb substituted Ba hexa-ferrite film have not been well understood.

In this study, we have investigated the crystallization mechanism of (Ba·Pb) hexa-ferrite thin films. We revealed that the low crystallization temperature of the (Ba·Pb) hexa-ferrite phase was due to the lower diffusion activation barrier of Pb cations than that of Ba cations.

2 Experimental procedure

(Ba·Pb) hexa-ferrite and Ba hexa-ferrite films were grown on sapphire (00*l*) substrates at room temperature by radio frequency (rf) magnetron sputtering of a stoichiometric (Ba·Pb)

hexa-ferrite and Ba hexa-ferrite target. As a carrier gas, a mixture of Ar-10% O_2 was used. Base pressure was 1×10^{-6} Torr and working pressure was 2×10^{-2} Torr. The rf power was 1 W/cm^2 and the deposition rate was about 4 Å/min. The deposited film thickness was ∼300 Å. To avoid the inhomogeneous sputtering, we performed pre-sputtering about 10 min. However, the Rutherford backscattering spectroscopy (RBS) data shows that the deposited films were deficient of Ba- and Pb component compared to Fe component. The composition of as-deposited (Ba·Pb) hexa-ferrite and Ba hexa-ferrite films were $(Ba_{0.55}Pb_{0.41})Fe_{12}O_{19}$ and $Ba_{0.8}Fe_{12}O_{19}$, respectively.

The real time synchrotron X-ray scattering experiments were performed at beamline 5C2 at Pohang Light Source in Korea. The experiments were carried out by measuring conventional longitudinal profiles ($\theta - 2\theta$ scan) and rocking curves (θ scan) in real time during annealing. The incident x rays were vertically focused by a mirror, and monochromatized to the wavelength of 1.38 Å by a double bounce Si (111) monochromator. The annealing temperature was raised step by step (Increasing rate: 20°C/min) and kept constant during the X-ray measurements (Measurement time: ∼20 min). Anomalous X-ray scattering (AXS) experiments were performed at the BESSRC beamline 11ID-D at Advanced Photon Soruce. The momentum transfer was fixed to the position of hexa-ferrite (00*l*) at each photon energy during the AXS measurements. For the AXS, the amorphous precursor films were annealed in *ex-situ*. The magnetic properties of the crystallized (Ba·Pb) hexa-ferrite and Ba hexa-ferrite films were measured using a vibrating sample magnetometer.

3 Results and discussions

We first present the longitudinal diffraction profiles of the (Ba·Pb) hexa-ferrite film measured at several temperatures during real time annealing. Figure 1(a) shows the diffraction profiles of (Ba·Pb) hexa-ferrite film (300 Å) during annealing. In the as-deposited film, there appeared a broad Bragg reflection at $\mathbf{q_z} = 2.592$ Å^{-1}, corresponding to the Fe_3O_4 (222) reflection (magnetite, JCPDS 19-0629). This indicated the existence of Fe_3O_4 crystalline phase in the sputter grown amorphous (Ba·Pb) hexa-ferrite films. It is noteworthy that the mosaic distribution of the Fe_3O_4 (222) phases was very small as 0.04° full width at half maximum (FWHM). This result implies that the Fe_3O_4 (222) phases were extremely well aligned on α-Al_2O_3 (00*l*) substrate as an interfacial phase.

As the annealing temperature increased to 450°C, the intensity of the Fe_3O_4 (222) reflection increased indicating that the interfacial Fe_3O_4 phase grew continuously. With increasing the annealing temperature further to 530°C, the intensity of Fe_3O_4 (222) reflection greatly decreased, while the Bragg reflection of the (Ba·Pb) hexa-ferrite (008) peak appeared at $\mathbf{q_z} = 2.161$ Å^{-1}. Above 630°C, the intensity of

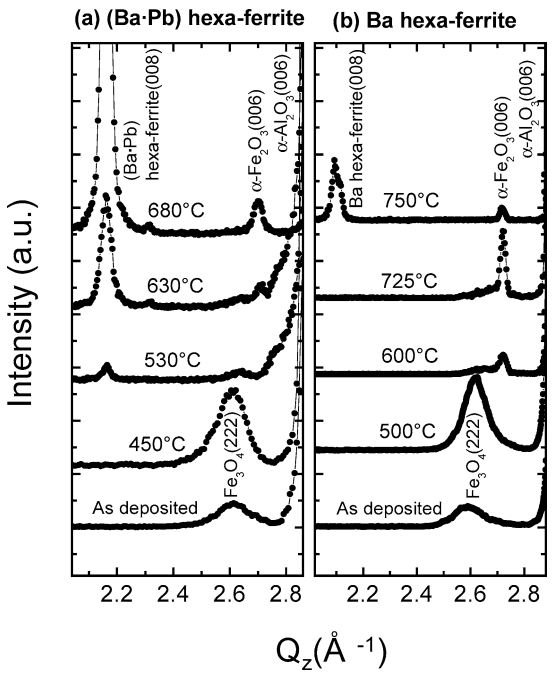

Fig. 1 X-ray longitudinal diffraction profiles of (a) the (Ba·Pb) hexa-ferrite and (b) the Ba hexa-ferrite film during real time annealing

the (Ba·Pb) hexa-ferrite (008) reflection increased significantly, and the Fe_3O_4 (222) reflection almost disappeared. This series of changes in the Bragg peak intensities suggests that the crystalline (Ba·Pb) hexa-ferrite phase be formed through the solid phase transformation of the crystalline interfacial Fe_3O_4 phase. The magnetite Fe_3O_4 phase has a close-packed structure of O anions; the close-packed layers are stacked in the ABCABC sequence in the [111] direction. The unit cell of the ferrimagnetic (Ba·Pb) hexa-ferrite also has a close-packed structure of O anions with a complicating stacking sequence (ABABCACACB) [7]. Therefore, it is possible that metal cations such as Pb and Ba diffuse into the (111) planes of Fe_3O_4 phase, resulting in the solid phase transformation of the Fe_3O_4 phase to the (Ba·Pb) hexa-ferrite phase. It is noteworthy that the crystallization temperature of (Ba·Pb) hexa-ferrite film was very low (∼530°C) compared to that of conventional Ba hexa-ferrite films (750–900°C).

It is also notable that the α-Fe_2O_3 phase was formed as a secondary phase during annealing. As previously discussed in experimental procedure, we used a stoichiometric (Ba·Pb) hexa-ferrite target and performed pre-sputtering to deposit homogeneous films. However, (Ba·Pb) components were short in the deposited film, resulting in the formation of the α-Fe_2O_3 phase at high temperature. As shown in the Fig. 1(a), α-Fe_2O_3 (006) grew as a secondary phase at high temperature (>630°C), due to deficiency of (Ba·Pb) components.

We also investigated the crystallization behavior of Ba hexa-ferrite film (∼300 Å) by measuring the longitudinal

profiles at several temperatures during annealing, as illustrated in Fig. 1(b). The crystallization of Ba hexa-ferrite film proceeded by two steps.

In the first step (at ∼600°C), the Bragg peak intensity of the Fe_3O_4 (222) reflection greatly decreased, while the Bragg reflection of α-Fe_2O_3 (006) peak appeared at $\mathbf{q_z} = 2.750\ \text{Å}^{-1}$. This indicated that the α-Fe_2O_3 (006) phase was formed by the solid phase transformation of the interfacial Fe_3O_4 (222) phase. (It was also extremely well aligned on the substrate). The phase transformation of Fe_3O_4 (111) to α-Fe_2O_3 (001) phase by oxidation was previously reported in the literature [8].

In the second step (at ∼750°C), the Ba hexa-ferrite (008) phase was crystallized by the transformation of the α-Fe_2O_3 (006) phase. It was previously reported that the Ba hexa-ferrite phase is formed by solid phase transformation of the α-Fe_2O_3 phase by the diffusion of Ba cations at high temperature (∼750°C) [9]. We note here that the (Ba·Pb) hexa-ferrite phase crystallized at much lower temperature (∼530°C) than the Ba hexa-ferrite phase (∼750°C). We speculated that the low crystallization temperature of the (Ba·Pb) hexa-ferrite phase was attributed to the lower diffusion activation barrier of Pb cations than that of Ba cations.

To investigate if the Pb cations play a crucial role in the low-temperature crystallization of (Ba·Pb) hexa-ferrite thin films, we performed AXS with the (Ba·Pb) hexa-ferrite thin film. For AXS study, the longitudinal diffraction scan was first performed to determine the peak position of the (Ba·Pb) hexa-ferrite (008) reflection ($\mathbf{q_z} = 2.161\ \text{Å}^{-1}$) at each X-ray energies [vicinity of the Ba L_I-edge (5.989 keV) and Pb L_{III}-edge (13.035 keV)]. Then, the momentum transfer was fixed to the position of the (Ba·Pb) hexa-ferrite (008) reflection and the scattering intensities were measured as the X-ray energy changed through Ba L_I-edge and Pb L_{III}-edge, respectively.

Figure 2 shows the AXS spectra of the (008) peak in the (Ba·Pb) hexa-ferrite thin film, which was annealed in *ex-situ* at 550°C for 2hr. The AXS spectra in the vicinity of the Ba L_I absorption edge showed no cusp, as shown in the Fig. 2(a). On the other hand, the AXS spectra near the Pb L_{III} absorption edge [Fig. 2(b)] showed a well defined cusp. If the element in question is associated with the Bragg peak, then the elemental absorption causes a decrease in the Bragg intensity, and a cusp appears near the absorption edge [10]. Therefore, the AXS spectra immediately indicated that there existed Pb cations in the hexa-ferrite phase at the low temperature of ∼550°C. Ba cations, however, were not observed in the crystallized hexa-ferrite phase.

We speculate that the Ba cations largely exist in the un-crystallized amorphous region of the films or probably even in grain boundaries of the crystallized phase, resulting in the disappearance of cusp. As shown in the Fig. 1(a), the film began to crystallize to the hexa-ferrite phase above ∼530°C. Therefore, the film was not fully crystallized and mostly composed of un-crystallized amorphous phase at the low annealing temperature of 550°C.

We suggest that the low crystallization temperature of the (Ba·Pb) hexa-ferrite phase was due to the lower diffusion activation barrier of Pb cations than that of Ba cations. The ionic radius of Pb cations is 1.40 Å smaller than that of Ba cations (1.61 Å) [11]. Pb is more volatile element than Ba [5] and Pb hexa-ferrite has much lower melting temperature (1315°C) compared to Ba hexa-ferrite (1565°C) [6]. Therefore, Pb cations can diffuse into the Fe_3O_4 phase more easily than Ba, resulting in the low temperature crystallization (< 550°C) of the (Ba·Pb) hexa-ferrite.

Figure 3 shows the hysteresis curves and SEM images of (a) (Ba·Pb) hexa-ferrite and (b) Ba hexa-ferrite. Interestingly the saturation magnetization (*Ms*) of the (Ba·Pb) hexa-ferrite film, 337 emu/cm^3, was larger than that of the Ba hexa-ferrite film, 241 emu/cm^3. We also note that the columnar type grain sizes of the crystallized (Ba·Pb) hexa-ferrite and the Ba hexa-ferrite films were comparable as ∼40nm in diameter, as shown in the SEM morphologies.

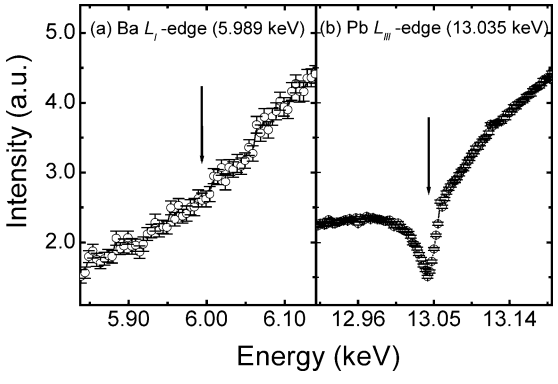

Fig. 2 The AXS spectra of the (008) peak in the (Ba·Pb) hexa-ferrite thin film (∼300 Å) that was annealed in *ex-situ* at 550°C for 2hr. The AXS spectra near (a) the Ba L_I-edge and (b) the Pb L_{III}-edge

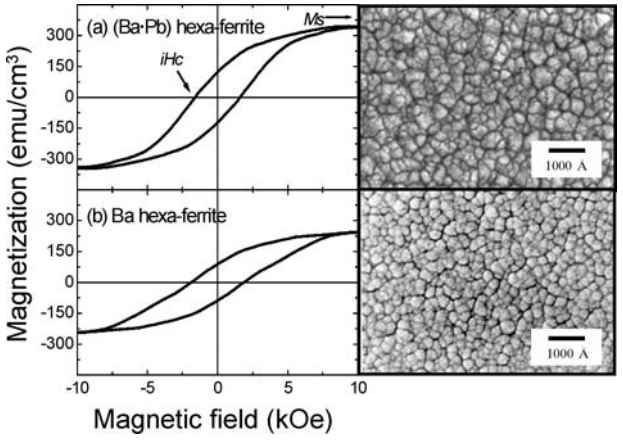

Fig. 3 Magnetic properties and surface morphologies of (a) the crystallized (Ba·Pb) hexa-ferrite and (b) the crystallized Ba hexa-ferrite film

These results suggest that the (Ba·Pb) hexa-ferrite film could be suitable for high-density magnetic recording media. The intrinsic coervity (*iHc*) values for the crystallized (Ba·Pb) hexa-ferrite and the Ba hexa-ferrite films were similar as 1.60 and 1.88 kOe, respectively.

As shown in Fig. 3, the *Ms* (337 emu/cm^3) of the (Ba·Pb) hexa-ferrite film in this study was larger than that (241 emu/cm^3) of the Ba hexa-ferrite film. Considering that Pb/Fe ratio in $(Ba_{0.55}Pb_{0.41})Fe_{12}O_{19}$ film was smaller than Ba/Fe ratio in $Ba_{0.8}Fe_{12}O_{19}$ film, we speculated that Ba component in (Ba·Pb) hexa-ferrite film contributed to the larger *Ms* of the (Ba·Pb) hexa-ferrite film. Therefore, it was concluded that the new crystallized phase was composed of (Ba·Pb) hexa-ferrite phase.

4 Conclusions

In conclusion, we revealed that the low crystallization temperature of the (Ba·Pb) hexa-ferrite phase (∼530°C) was due to the lower diffusion activation barrier of Pb cations than that of Ba cations. The crystalline (Ba·Pb) hexa-ferrite phase was formed by solid phase transformation of the interfacial crystalline Fe_3O_4 phase through the diffusion of Ba and Pb cations. The small grain size (∼40nm in diamter) and comparable magnetic properties ($Ms_\perp$: 337 emu/cm^3, $iHc_\perp$: 1.60 kOe) of the crystallized (Ba·Pb) hexa-ferrite film demonstrated its potential possibility for high-density recording media.

Acknowledgment We acknowledge the support of the BK 21 Project and MOST(KOSEF) through the National Research Laboratory (NRL) project.

References

1. T.L. Hylton, M.A. Parker, M. Ullah, K.R. Coffey, R. Umphress, and J.K. Howard, *J. Appl. Phys.*, **75**, 5960 (1994).
2. X. Sui and M.H. Kryder, *Appl. Phys. Lett.*, **63**, 1582 (1993).
3. W.H. Von Aulock, *Handbook of Microwave Ferrite Materials* (Academic, London, 1965).
4. T.L. Hylton, M.A. Parker, and J.K. Howard, *Appl. Phys. Lett.*, **61**, 867 (1992).
5. P.C. Dorsey, S.B. Qadri, K.S. Grabowski, D.L. Knies, P. Lubitz, D.B. Chrisey, and J.S. Horwitz, *Appl. Phys. Lett.*, **70**, 1173 (1997).
6. A. Morisako, H. Nakanishi, and M. Matsumoto, *J. Appl. Phys.*, **75**, 5969 (1994).
7. B.D. Cullity, *Introduction to Magnetic Materials* (Addison-Wesley, Reading, MA, 1972), Chap. 6.
8. S.J. Doh, J.H. Je, and T.S. Cho, *J. Cryst. Growth.*, **240**, 355 (2002).
9. T.S. Cho, J.H. Je, and D.Y. Noh, *Appl. Phys. Lett.*, **76**, 303 (2000).
10. H. Stragier, J.O. Cross, J.J. Rehr, L.B. Sorensen, C.E. Bouldin, and C.E. Woicik, *Phys. Rev. Lett.*, **69**, 3064 (1992).
11. David R. Lide, *CRC Handbook of Chemistry and Physics* 12–8, 74th edition (CRC PRESS, INC., 1993–1994).